MicroRNA-874-3p/ADAM (A Disintegrin and Metalloprotease) 19 Mediates Macrophage Activation and Renal Fibrosis After Acute Kidney Injury

Article *in* Hypertension · March 2021

DOI: 10.1161/HYPERTENSIONAHA.120.16900

14 authors, including:

Xishao Xie
Zhejiang University
25 PUBLICATIONS **196** CITATIONS
SEE PROFILE

Weiqiang Lin
Zhejiang University
53 PUBLICATIONS **879** CITATIONS
SEE PROFILE

Hypertension

KIDNEY

MicroRNA-874-3p/ADAM (A Disintegrin and Metalloprotease) 19 Mediates Macrophage Activation and Renal Fibrosis After Acute Kidney Injury

Junni Wang,* Wanyun Nie,* Xishao Xie,* Mengqiu Bai, Yanhong Ma, Lini Jin, Liang Xiao, Peng Shi, Yi Yang, Pedro A. Jose, Ines Armando, Jianghua Chen, Weiqiang Lin, Fei Han

ABSTRACT: Inflammation and maladaptive repair play a crucial role in the development of chronic kidney disease and hypertension after acute kidney injury. To study the mechanisms involved in acute kidney injury-to-chronic kidney disease transition, we established a chronic renal fibrosis mouse model that was triggered by an initial ischemia/reperfusion–induced acute kidney injury (acute-chronic model). Downregulation of microRNA-874-3p during renal fibrosis was identified by a genome-wide RNA-sequencing and was further confirmed in cell-based assays, mouse models, and human samples. Overexpression of microRNA-874-3p in the kidneys markedly alleviated renal fibrosis, accompanied with decreased infiltrated macrophages and expression of α-smooth muscle actin, type I collagen, fibronectin, CCL (C-C motif chemokine ligand) 2, and ADAM (A Disintegrin and Metalloprotease) 19. *ADAM19* is a target gene of microRNA-874-3p as shown by luciferase reporter assays and was upregulated in the acute-chronic model. Overexpression of ADAM19 directly induced the expression of fibrotic genes, CCL2, and macrophage infiltration in vivo. Depletion of macrophages using clodronate liposomes ameliorated the fibrogenic effects of ADAM19. Overexpression of ADAM19 also induced accumulation of the Notch1 intracellular domain, an upstream regulator of CCL2 expression, whereas Notch1 pathway antagonist N-(N-[3,5-difluorophenacetyl]-L-alanyl)-S-phenylglycine t-butyl ester reduced CCL2 level in ADAM19-overexpressed cells. Collectively, microRNA-874-3p/ADAM19 mediates renal fibrosis after acute kidney injury by increasing macrophage infiltration via the Notch1/CCL2 pathway. (***Hypertension*. 2021;77:1613–1626. DOI: 10.1161/HYPERTENSIONAHA.120.16900.)** • **Data Supplement**

Key Words: fibrosis ■ inflammation ■ kidney ■ macrophage

Chronic kidney disease (CKD) is a common cause of hypertension, due to sympathetic nervous system and renin-angiotensin-aldosterone system overactivity, extracellular volume expansion, endothelial dysfunction, immune activation, and inflammation.[1,2] As one of the major underlying mechanisms shared in hypertension and CKD, renal inflammation, and fibrosis profoundly affect the clinical outcomes of patients. Accumulated evidence has implicated a role of renal immune activation in virtually all aspects of the development of CKD and hypertension. This includes leading inflammatory cell infiltration, production cytokines, reactive oxygen species and other factors, dysfunctional sodium and water handling, alterations in vascular resistance, and eventual end-organ remodeling and damage.[3] However, the onset of this process remains incompletely understood.

Observational studies have suggested a strong association between acute kidney injury (AKI; even a minor injury) and the subsequent development of CKD.[4] In a considerable proportion of patients with AKI, in

Correspondence to: Fei Han, Kidney Disease Center, The First Affiliated Hospital, Zhejiang University School of Medicine, Zhejiang Province, Hangzhou 310003, China, Email hanf8876@zju.edu.cn or Weiqiang Lin, Kidney Disease Center, The First Affiliated Hospital, Institute of Translational Medicine, Zhejiang University School of Medicine, Hangzhou 310003, China, Email wlin@zju.edu.cn

*J. Wang, W. Nie and X. Xie contributed equally.

The Data Supplement is available with this article at https://www.ahajournals.org/doi/suppl/10.1161/HYPERTENSIONAHA.120.16900.

For Sources of Funding and Disclosures, see page 1625.

Hypertension is available at www.ahajournals.org/journal/hyp

Novelty and Significance

What Is New?

- MicroRNA (MiR)-874-3p/ADAM (A Disintegrin and Metalloprotease) 19 mediates renal fibrosis after acute kidney injury by increasing macrophage infiltration via the Notch1/CCL2 pathway.
- MiR-874-3p suppresses CCL2 expression and macrophage infiltration and attenuates renal fibrosis by decreasing ADAM19, strongly suggesting a therapeutic potential for miR-874-3p in the treatment of renal fibrosis.
- MiR-874-3p expression in peripheral blood mononuclear cells of IgA nephropathy patients with severe classes was decreased, along with increased expression of ADAM19 in the kidney of the same human cohort, indicating that miR-874-3p could also serve as a blood marker to detect renal fibrosis.
- High ADAM19 expression directly leads to renal inflammation and renal fibrosis, and it induces the formation of NICD1 (Notch receptor intracellular domain 1), indicating that ADAM19 can activate Notch1.

What Is Relevant?

- The progression of kidney damage and hypertension is closely related to renal histological fibrosis in chronic kidney disease patients.
- Here, we show that the miR-874-3p/ADAM19 pathway regulates renal fibrogenesis after acute kidney injury.

Summary

MiR-874-3p/ADAM19 mediates renal fibrosis after acute kidney injury by increasing macrophage infiltration via the Notch1/CCL2 pathway. These findings not only provide new insights into the mechanisms underlying renal fibrosis but also offer potential therapeutic targets for treating this disease.

Nonstandard Abbreviation and Acronyms

ADAM	A Disintegrin and Metalloprotease
AKI	acute kidney injury
CCL	C-C motif chemokine ligand
CKD	chronic kidney disease
Fn	fibronectin
GFP	green fluorescent protein
I/R	ischemia/reperfusion
IgAN	IgA nephropathy
KIM-1	kidney injury molecule-1
NC	negative control
PBMC	peripheral blood mononuclear cells
qPCR	quantitative polymerase chain reaction
RNA-seq	RNA-sequencing
TGF	transforming growth factor
UTR	untranslated region
UUO	unilateral ureteral obstruction
α-SMA	α-smooth muscle actin

spite of no previous evidence of kidney disease, renal function recovers only partially, which is followed by a gradual progression toward end-stage renal disease with the development of hypertension.[5–7] In a cohort study of children previously treated with extracorporeal membrane oxygenation, history of AKI was associated with high risk of hypertension during long-term follow-up.[8] Maladaptive repair and tissue regeneration after AKI may cause a series of pathophysiological changes, such as systemic and intrarenal hypertension, glomerular hyperfiltration, progressive glomerulosclerosis, and tubulointerstitial fibrosis. All of the activation of these mechanisms involved in AKI-to-CKD transition can be independent of the cause of AKI.[9]

MicroRNAs (miRNAs) are single-stranded small noncoding RNAs with a length of about 22 nucleotides. By targeting mRNA degradation or inhibiting translation, miRs regulate diverse biological processes,[10,11] including those that occur in AKI or CKD.[11–18] Although many miRs in kidney fibrosis have been identified in the past decade, very few studies have assessed the role of miRs in AKI-to-CKD transition.[13,19] To study this, we established a mouse model of AKI-to-CKD transition (referred to as acute to chronic or acute-chronic [AC] model). Genome-wide RNA-sequencing revealed that miR-874-3p and one of its downstream targets, ADAM (A Disintegrin and Metalloprotease) 19, are involved in this critical process.

ADAM19 is a membrane-anchored glycoprotein of ADAM family, which contains multiple extracellular catalytic domains. It has been shown to modulate cell-cell and cell-matrix interactions, activate cell proliferation, and generate soluble and active forms of proteins by cleaving transmembrane proteins nearby.[20,21] ADAM19 is widely expressed in embryos and plays an essential role in organ development. *Adam19*-deficient mice could not survive the perinatal period due to cardiac insufficiency.[21,22] In adults, ADAM19 is moderately expressed in normal kidneys. However, upregulation of ADAM19 has been documented in almost all renal diseases, including IgA nephropathy (IgAN) and hypertensive nephropathy.[20,23] Despite this observation, roles of ADAM19 in renal fibrosis have not been investigated.

Based on our genome-wide RNA-sequencing results, we tested the hypothesis that miR-874-3p plays a crucial role in AKI-to-CKD transition via regulating ADAM19. MiR-874-3p suppressed CCL2 expression and macrophage infiltration and attenuates renal fibrosis by decreasing ADAM19. Overexpression of ADAM19 alone in kidneys led to macrophage infiltration and fibrosis. Mechanistically, ADAM19 caused accumulation of the Notch1 intracellular domain, an upstream regulator of CCL2 expression. Our findings identify a new mechanism underlying the pathogenesis of renal fibrosis and provide new potential therapeutic targets for treating renal fibrosis after AKI.

METHODS

The data that support the findings of this study are available from the corresponding author upon reasonable request.

Human Kidney and Blood Samples

All patients were recruited in the Kidney Disease Center of the First Affiliated Hospital of Zhejiang University. This research protocol conformed to the provisions of the Declaration of Helsinki and was approved by the Ethics Committee of the First Affiliated Hospital of Zhejiang University. The diagnosis of IgAN was based on renal biopsies. No patient received immunosuppressive treatment before the renal biopsy. Clinical characteristics of the patients at biopsy are shown in Table S1 in the Data Supplement. Peripheral blood mononuclear cells for miR-874-3p quantitative polymerase chain reaction (qPCR) analysis were isolated from whole-blood samples collected at the time of biopsy. The renal tissues were used for the immunohistochemistry of ADAM19 expression. Lee classification of IgAN[24] was shown in the Data Supplement.

Animal Models

Male C57BL/6J mice at 8 to 10 weeks of age weighing 20 to 25 g were purchased from Shanghai SLAC Laboratory. Mice were housed in specific-pathogen-free environment, with a 12-h light/dark cycle, in the animal facility of Zhejiang University. All animal studies were approved by the Committees for Animal Experiments of Zhejiang University and were performed according to the institutional guidelines of Zhejiang University in China.

Ischemia/Reperfusion–Induced Renal Fibrosis (AC Model) in Mice

AC model was induced, as previously described.[25,26] Briefly, under anesthesia, the left renal artery and vein were exposed and clamped for 30 minutes. After releasing the clip for blood reperfusion, the incision was sutured. During the surgery, the body temperature of the mice was kept between 36 °C and 38 °C, using an electric heating blanket. A right nephrectomy was performed the day before euthanizing the mice to assess the left renal function. We euthanized mice and harvested kidneys 5 or 10 days after ischemia/reperfusion (I/R). For further validation, we also performed a time-course study on AKI-to-CKD transition with kidneys harvested on day 2, 6, 8, 14, and 28. Sham-operated mice served as controls (Figure S1A).

Unilateral Ureteral Obstruction in Mice

To confirm the findings with another renal fibrosis model, unilateral ureteral obstruction (UUO) was performed as described previously.[27] In brief, after anesthesia with 60 mg/kg sodium pentobarbital, the left ureter of the mouse was exposed and ligated, and the left kidney was harvested at different time points after surgery, depending on the experiment's requirement. Sham-operated mice served as controls (Figure S1A).

Microinjection of Adenovirus into Mouse Kidney

Based on preliminary study, we designed an adenoviral vector encoding GFP (green fluorescent protein)-labeled miR-874-3p (Vigene Biosciences) or ADAM19 (GeenChem). Adenoviruses or empty vectors were administered to mice according to a published method.[28] Briefly, multipoint in situ injection of adenovirus with 33G microsyringe (Hamilton) into the left kidney of mice was performed 4 days before UUO or I/R surgery. The details are listed in the Data Supplement.

Cell Culture and Treatments

A human renal proximal tubular epithelial cell line (HK2), a rat renal proximal tubular epithelial cell line (NRK-52E), and human embryonic kidney cell line (293T) were purchased from the American Type Culture Collection. NRK-52E, 293T cells were grown in DMEM (GIBCO 12430) supplemented with 10% FBS (GIBCO 10099) and 1% penicillin/streptomycin (GIBCO 15140). HK2 cells were grown in RPMI 1640 medium (Sigma) with 10% FBS and 1% penicillin/streptomycin. All cells were cultured in a 37 °C incubator containing 5% CO_2. In some experiments, the cells were plated into 6-well or 12-well plates and incubated with the recombinant TGF (transforming growth factor)-β1 (10 ng/mL, R&D Systems) or N-[N-(3,5-Difluorophenacetyl)-L-alanyl]-S-phenylglycine t-butyl ester (10 mmol/L, Selleck). Lipofectamine 3000 Transfection Reagent (Invitrogen) was used in the transfection of miR mimics, inhibitors (RiboBio), and siRNA oligos (GenePharma), according to the manufacturer's instructions.

Luciferase Reporter Assay

As described previously,[29] two 500 bp fragments of DNA containing 2 predicted miR-874-3p binding sites located in the 3′-UTR region of human *ADAM19* gene were cloned into psi-CHECK-2 vector, respectively. The clones were sequenced to the sites that were mutated. The *ADAM19* untranslated region (UTR) plasmid or mutated plasmids were cotransfected with miR-874-3p mimics or negative control (NC) into 293T cells. The dual-luciferase reporter assay was performed with the Dual-Luciferase Reporter Assay Kit (Promega E1910) following the manufacturer's instructions.

RNA Extraction and qPCR Analysis

With cultured cells and kidney tissues collected and homogenized, RNA was extracted using ESscience RNA-Quick Purification Kit (YiShan Biotech, Shanghai, China). RNA samples were reverse transcribed for mRNA level quantification via qPCR using HiScript III RT SuperMix and qPCR Master Mix (Vazyme). Primers for qPCR are listed in Table S4. The bulge-loop miRNA reverse transcription and qPCR primer sets (one reverse transcription primer and a pair of qPCR primers for

each set) specific for miR-874-3p are designed by RiboBio (Guangzhou, China). U6 small nuclear RNA was used as control for miR-874-3p qPCR.

RNA Deep Sequencing and Data Analysis

The kidneys from the UUO model group, AC model group, and sham group obtained 5 days after surgery were used for total RNA extraction. Three mice were included in each group. The total RNA was subjected to RNA-sequencing (RNA-seq) to determine miRNA and mRNA expression patterns. We also conducted RNA-seq in the UUO mice that were microinjected with miR-874-3p or empty virus; each group had 4 mice. Bioinformatics analyses including raw data process, differential gene expression analysis, and Kyoto Encyclopedia of Genes and Genomes analysis were conducted by Anoroad and HaploX Genomic Center.

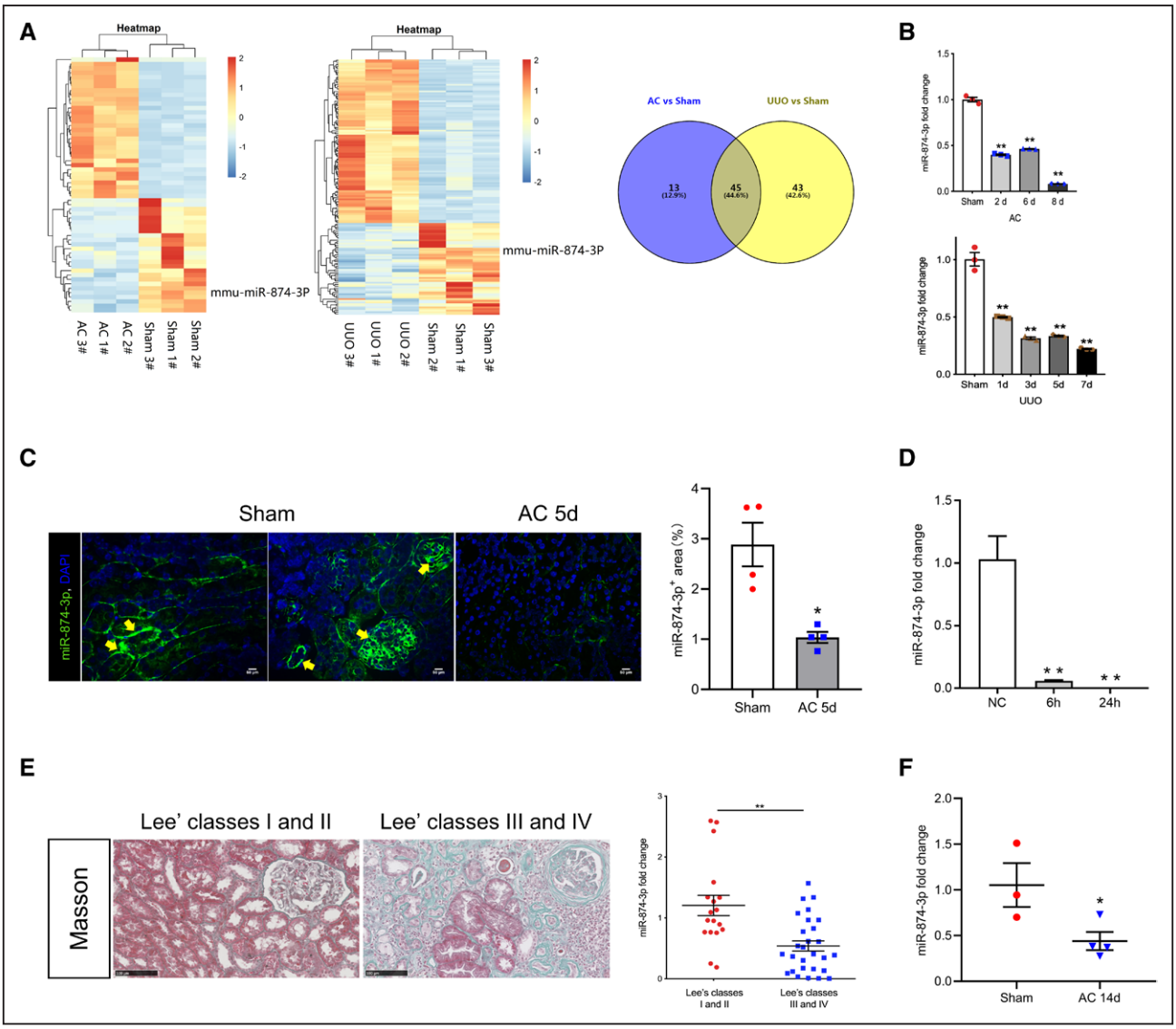

Figure 1. MicroRNA (MiR)-874-3p expression is reduced in renal fibrosis.

A, Heatmaps of the differentially expressed miRs in kidneys of acute-chronic (AC) and unilateral ureteral obstruction (UUO) mice and their respective controls. Venn diagram of differentially expressed miRNAs in the kidney of AC, and UUO mice. Forty-five differentially expressed miRNAs were found in the kidney of both mouse models. **B**, Renal expression of miR-874-3p decreased early (2 d) and remained decreased (6 d, 8 d) in AC mice. The trend was also observed in UUO mice. n=3 for sham, AC and UUO groups at each time point. $^{**}P<0.01$ vs sham. **C**, Fluorescence in situ hybridization in kidneys of mice showed that miR-874-3p expression in kidney (yellow arrows) was reduced in AC mice at day 5. Scale bar, 50 μm. Quantification of miR-874-3p staining in renal tissues showed miR-874-3p expression decreased in AC mice at day 5. n=4 for sham and AC groups, $^{*}P<0.05$. **D**, Treatment of HK2 cells with TGF (transforming growth factor)-β1 (10 ng/mL) for 6 or 24 h markedly decreased miR-874-3p expression. n=3 for each group, $^{**}P<0.01$ vs NC. **E**, Masson trichrome staining of renal biopsy samples of IgA nephropathy patients showed severe renal fibrosis in patients with Lee class III and IV. quantitative polymerase chain reaction analysis of miR-874-3p expression in peripheral blood mononuclear cells of IgA nephropathy patients (18 patients graded as Lee class I and II vs 29 patients with Lee class III and IV) showed miR-874-3p was significantly lower in patients with Lee class III and IV. $^{**}P<0.01$. **F**, MiR-874-3p expression in mouse peripheral blood mononuclear cells was decreased in renal fibrosis. Sham, n=3; AC group, n=4; $^{*}P<0.05$. Data were expressed as means±SEM. Student *t* test was for (**C**) and (**F**), Mann-Whitney *U* test was used for (**E**), and One-way ANOVA and Tukey post hoc test were used for (**B**) and (**D**).

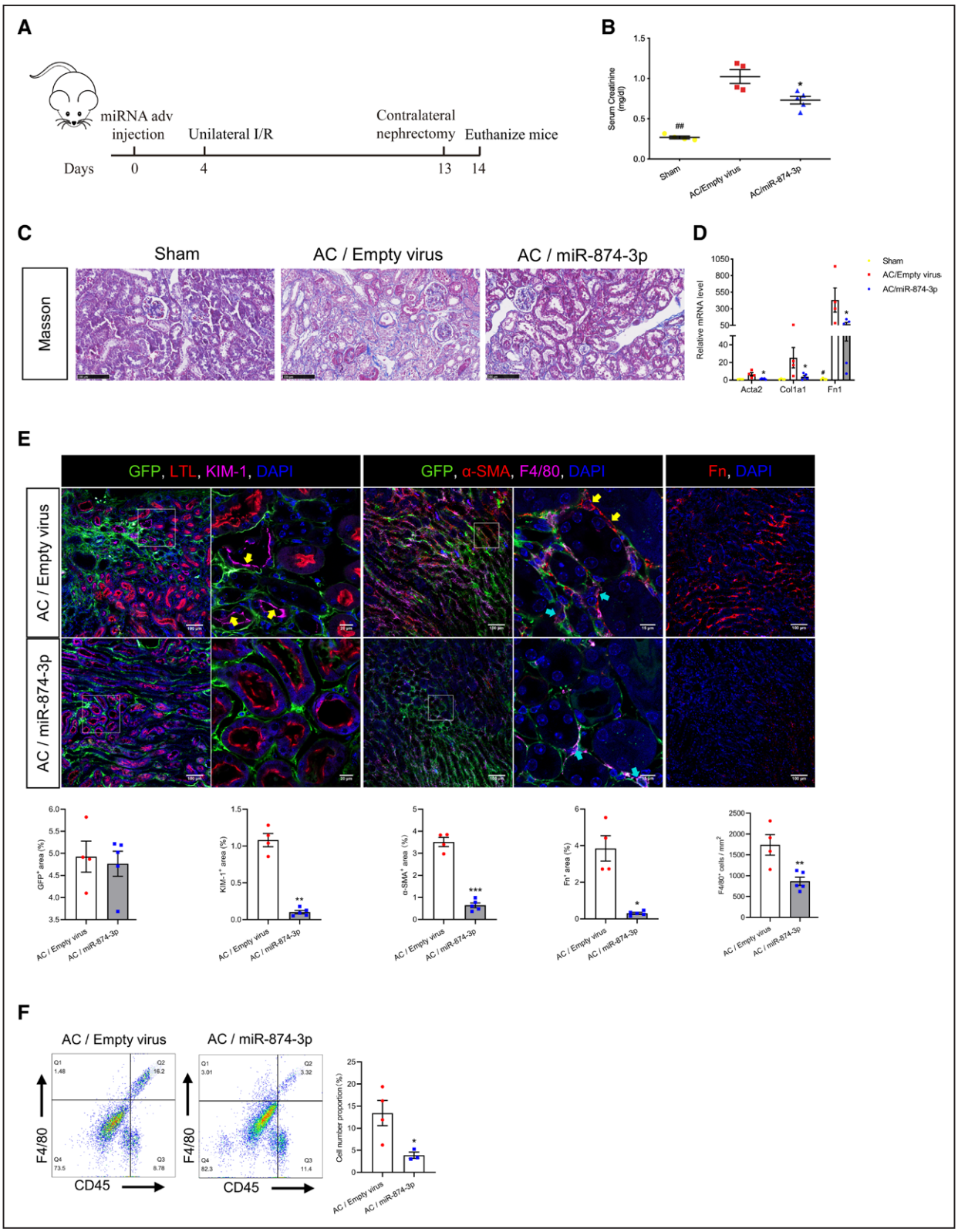

Figure 2. MicroRNA (MiR)-874-3p reduces renal fibrosis in the acute-chronic (AC) model.
A, Schematic diagram for experimental design. GFP (green fluorescent protein)-labeled adenoviruses carrying human *miR-874-3p* or empty viruses were delivered to mice through kidney injection 4 days before ischemia/reperfusion (I/R) surgery. **B**, Serum creatinine of mice treated with miR-874-3p virus was lower than in mice treated with empty virus, but both were higher than in sham-operated mice. Sham, n=4; empty virus, n=4; miR-874-3p group, n=5; ##P<0.01, sham vs all; *P<0.05, miR-874-3p vs all. **C**, Masson trichrome staining of renal sections showed decreased areas of fibrosis in AC mice treated with miR-874-3p virus than in mice treated with empty virus. Scale bar, 100 μm. **D**, Overexpression of miR-874-3p in the kidney decreased the renal mRNA expression of *Acta2, Col1a1,* (*Continued*)

Mouse Kidney Cells Flow Cytometry

Mouse kidneys were harvested after cold PBS perfusion. Kidney samples were mechanically minced and then digested in RPMI 1640 (Corning) with 1.5 mg/mL collagenase IV (Worthington) and 100 Unit DNase I (Sigma) for 30 minutes at 37 °C. Then, cells were filtered through a 70 μm cell strainer (Biologix). Inflammatory cells in kidneys were further enriched by Percoll gradient centrifugation (700*g*, room temperature, 20 minutes without brake). The middle layer from 36/72% percoll was collected and washed with PBS. After centrifugation (300*g*, 4 °C, 5 minutes), cells were counted and plated into 96-well for further staining.

Cell suspension was incubated with Fc blocker (BioLegend) at 4 °C for 15 min. For surface antigens staining, antibody cocktails were added to cells at 4 °C in the dark for 20 minutes. For intracellular staining, cells were fixed by Fixation Buffer (BioLegend) at room temperature in the dark for 15 minutes. Neutralizing the Fixation Buffer leftover by incubating cells in Intracellular Staining Perm Wash Buffer (BioLegend) in the dark at room temperature for 5 minutes twice. Intracellular antigens were stained by antibody cocktails in Intracellular Staining Perm Wash Buffer in the dark for 40 minutes. Flow cytometry data were acquired on NovoCyte Flow Cytometer 2060R. Data were analyzed by FlowJo_vX.0.7.

Quantification and Statistical Analysis

Quantification of immunoblotting and immunostaining were analyzed with Image-Pro Plus version 6.0 (Media Cybernetics, Inc) and Image J version 1.52v (Rawak Software, Inc), as described previously.[30] All statistical analyses were performed using SPSS version 22.0 (SPSS, Inc). Continuous variables of clinical characteristics were presented as the means, and the SDs or the medians with the range depending on the distribution; categorical variables are presented as frequencies with percentages. Other data were expressed as means±SEM. The normal distribution of values was determined by Kolmogorov-Smirnov Test. Significant differences between and among groups were determined with Student *t* test, 1-way ANOVA, Mann-Whitney *U* test, or χ^2 test as appropriate. $P<0.05$ was considered statistically significant.

RESULTS

Renal Fibrosis Is Associated With miR-874-3p Downregulation

With protocol shown in Figure S1A, significant renal fibrosis and marked elevation of serum creatinine were observed in AC mice, and the same pattern of fibrosis was observed in cortex and medulla (Figure S1B and S1C). Similar renal fibrosis was also found in UUO mice (Figure S1C). Genome-wide RNA-Seq detected a total of 45 miRs that were differentially expressed in both models compared with sham (Figure 1A, Tables S2 and S3). Among all detected miRs, significant downregulation of miR-874-3p was confirmed by qPCR in both AC and UUO mice (Figure 1B and Figure S1D). Additional qPCR indicated that this phenomenon persisted over 28 days in AC mice (Figure S2). Moreover, fluorescence in situ hybridization revealed that miR-874-3p was widely expressed in kidney, including renal tubules, glomeruli, and interstitial cells, and the fluorescence was markedly compromised in samples from AC mice (Figure 1C). Furthermore, miR-874-3p was significantly decreased in HK2 cells treated with TGF-β1, a potent profibrotic factor, as determined by qPCR analysis (Figure 1D). Beside kidney cells, miR-874-3p was also found in human and mouse peripheral blood mononuclear cells (PBMCs). In patients with IgAN, a type of CKD accompanied by renal fibrosis, miR-874-3p was significantly lower in PBMCs in patients with Lee class III and IV than those with Lee class I and II (Figure 1E). Similar change was found in PBMCs from AC mice (Figure 1F). In parallel, the mean arterial pressure of the patients with Lee class I and II was significantly lower than that of grade III and IV patients (44.8% had hypertension; Table S1).

MiR-874-3p Reduces the Degree of Renal Fibrosis and Macrophage Infiltration

To investigate the role of miR-874-3p in vivo, we designed adenoviral vectors carrying human *miR-874* sequence (miR-874-3p mimic) with empty vectors used as controls. A GFP reporter under the same promoter with *miR-874* was included in the vector as shown in the diagram in Figure S3A. The expression of mature miR-874-3p was confirmed by qPCR (Figure S3B), and GFP$^+$ cells were detected in the kidney under confocal microscope. The expression of GFP in kidney was widespread at day 4, peaked at day 6, and lasted for 15 days (Figure S3C). GFP was detected primarily in interstitial cells (Figure S3C) and can also be found in renal tubules (Figure S3D). Administration of miR-874-3p mimic viral vector into mice 4 days before I/R (Figure 2A) attenuated the increases in serum creatinine (Figure 2B) and renal fibrosis (Figure 2C). The mRNA expressions of *Acta2* (α-smooth muscle actin, α-SMA), *Col1a1* (type I collagen), and *Fn1* (fibronectin, Fn) were

Figure 2 Continued. *Fn1* (fibronectin 1) in AC mice. Sham, n=4; empty virus, n=4; miR-874-3p, n=5; #$P<0.05$, miR-874-3p group vs sham; *$P<0.05$, miR-874-3p group vs empty virus. **E**, Representative images of immunofluorescence showed decreased staining of α-SMA (α-smooth muscle actin; red, yellow arrows) and Fn (red) in interstitial area, with less infiltration of F4/80$^+$ cells (violet, aqua arrows) in AC mice overexpressing miR-874-3p in kidney than in empty virus (GFP, green). LTL (lotus tetragonolobus lectin, red) labeled renal proximal tubules. KIM-1 (violet, yellow arrows) marked injured tubules. DAPI (blue) is a stain for nucleic acid. Scale bar, 100 μm, 20 μm and 15 μm. Quantification of immunostaining showed expression of KIM-1, α-SMA, Fn, and F4/80 decreased in AC mice treated with miR-874-3p virus. Empty virus, n=4; miR-874-3p, n=5; *$P<0.05$, **$P<0.01$, ***$P<0.001$. **F**, Flow cytometry analysis showed decreased renal macrophage infiltration in mice treated with miR-874-3p adenovirus. n=4 for empty virus and n=3 for miR-874-3p. *$P<0.05$. Data were expressed as means±SEM. Student *t* test was used for (**E**) and (**F**), One-way ANOVA and Tukey post hoc test were used for (**B**) and (**D**). miRNA adv indicates adenoviral vectors carried human microRNA-874-3p sequence.

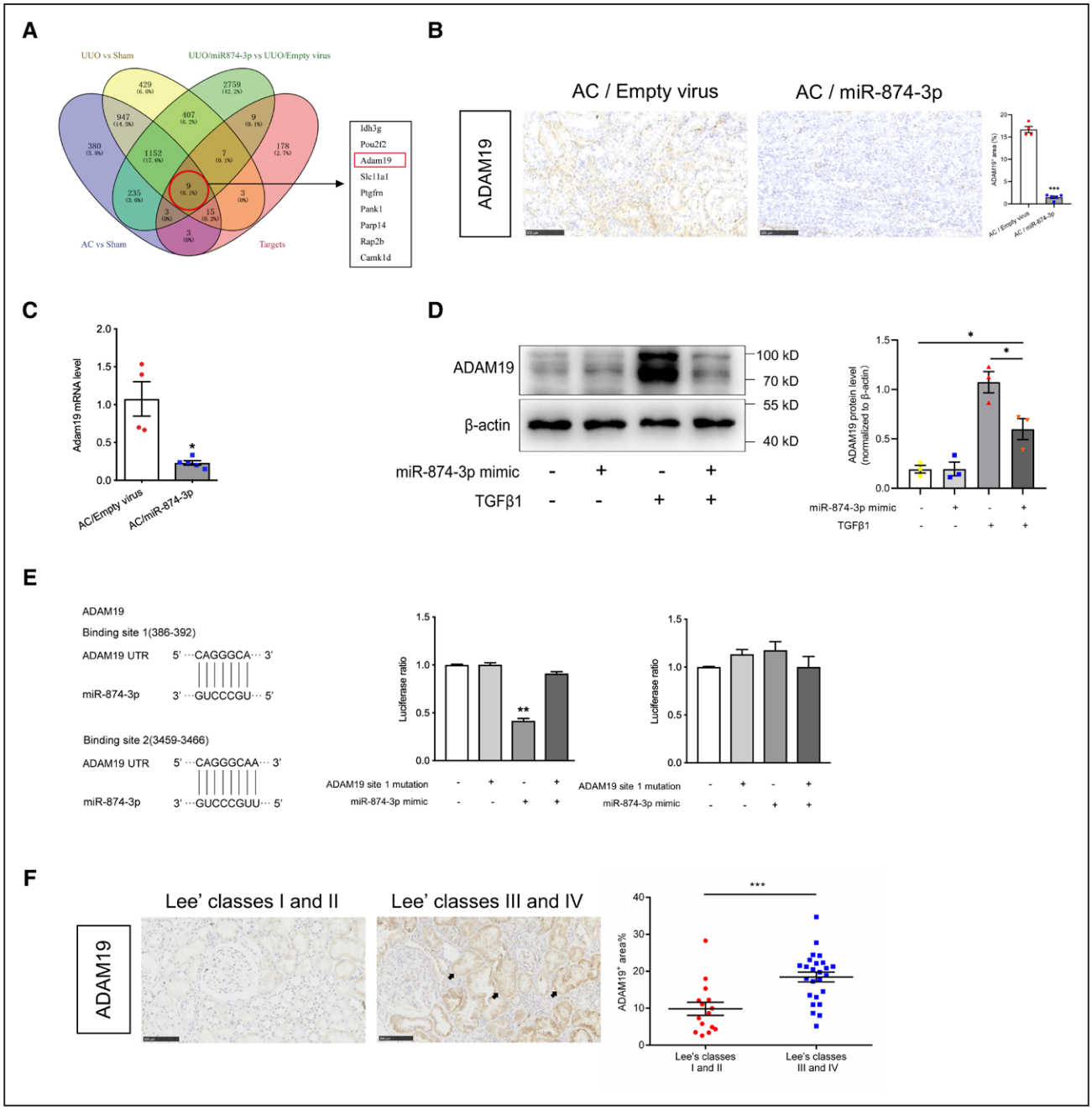

Figure 3. MicroRNA (MiR)-874-3p targets ADAM (A Disintegrin and Metalloprotease) 19 in renal fibrosis.
A, Venn diagram of differentially expressed mRNAs in acute-chronic (AC) model, unilateral ureteral obstruction (UUO) model, UUO model treated with miR-874-3p adenovirus, and miR-874-3p target database. **B**, Representative images of immunohistochemical staining showed less ADAM19 staining in AC mice treated with miR-874-3p adenovirus than in mice treated with empty virus. Scale bar, 100 μm. Quantification of immunostaining showed ADAM19 expression decreased in AC mice treated with miR-874-3p virus. Empty virus, n=4; miR-874-3p, n=5; ***P<0.001. **C**, Quantitative polymerase chain reaction showed decreased *Adam19* mRNA expression in AC mice treated with miR-874-3p adenovirus, relative to mice treated with empty virus. Empty virus group, n=4; miR-874-3p group, n=5 in AC model, *P<0.05 vs empty virus group. **D**, The increase in ADAM19 protein expression induced by TGF (transforming growth factor) β1 stimulation in HK2 cells was reduced in the presence of miR-874-3p mimic. The relative protein level was analyzed by gray levels and normalized by β-actin. n=3 for each group, *P<0.05. **E**, Luciferase microRNA target reporter assay showed that miR-874-3p targeted site 1 in the 3′-UTR of *ADAM19*. Normal plasmid served as control. n=3 for each group, **P<0.01 vs control group (empty bar). **F**, Representative images of immunohistochemical staining showed more ADAM19 staining (arrows) in renal biopsy samples of IgAN patients with Lee class III and IV than patients with Lee class I and II. Scale bar, 100 μm. Quantification of ADAM19 staining in renal biopsy samples of IgAN patients (15 patients graded as Lee classes I and II vs 25 patients with Lee classes III and IV) showed ADAM19 increased in patients with classes III and IV. ***P<0.001. Data were expressed as means±SEM. Student t test was for (**B**), (**C**), and (**F**). One-way ANOVA and Tukey post hoc test were used for (**D**) and (**E**).

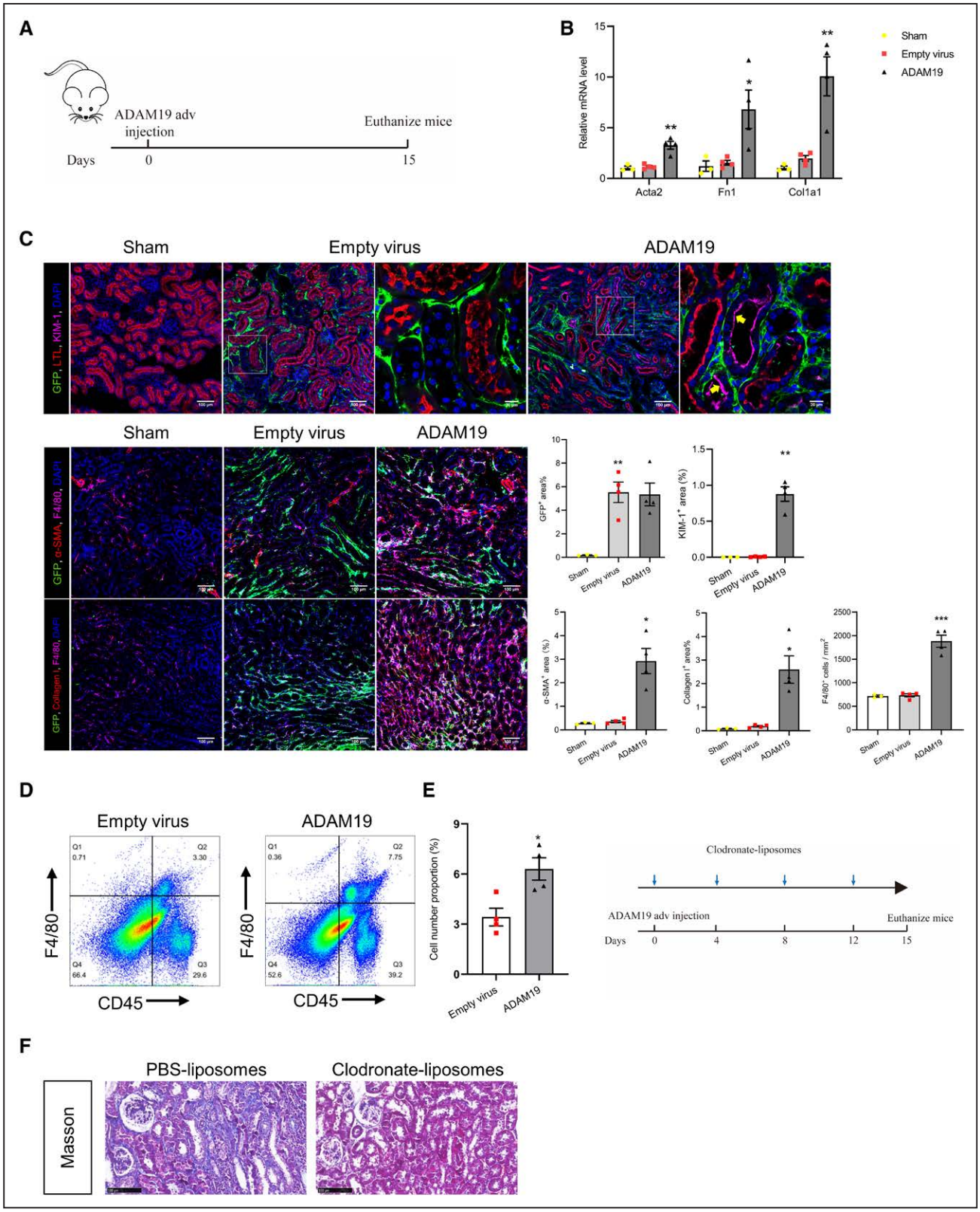

Figure 4. ADAM (A Disintegrin and Metalloprotease) 19 induces macrophage infiltration to promote renal fibrogenesis.
A, Schematic diagram for experimental design. Adenoviruses carrying mouse *Adam19* or empty viruses were delivered to mice through kidney injection. **B**, Overexpression of ADAM19 in the kidney increased the renal mRNA expressions of *Acta2, Col1a1,* and *Fn1* (fibronectin 1). Sham, n=3; ADAM19 and empty virus, n=4/group. **P*<0.05, ***P*<0.01, ADAM19 vs sham or empty virus. **C**, Representative images of immunofluorescence showed overexpression of ADAM19 (GFP [green fluorescent protein], green) led to more staining of α-SMA (α-smooth muscle actin; red), Col-I (red), F4/80 (violet) in tubulointerstitial area. LTL (lotus tetragonolobus lectin; red) (*Continued*)

decreased by 80%, 85%, and 84%, respectively, compared with mice that received empty viruses (Figure 2D). Overexpression of miR-874-3p in kidney decreased the staining of KIM-1 (kidney injury molecule-1), α-SMA, Fn, and F4/80 in mice treated with miR-874-3p mimic (Figure 2E and S4). As determined by flow cytometry analysis of mouse kidneys, macrophage infiltration was reduced in AC mice treated with miR-874-3p mimic (Figure 2F). To confirm the findings in a second model, we performed UUO in mice 4 days after miR-874-3p mimic or control transduction, and the results were similar to what we have found in AC model (Figure S5).

MiR-874-3p Targets ADAM19 in Renal Fibrosis

RNA-Seq was performed to identify differentially expressed genes in UUO mice treated with miR-874-3p mimic in comparison with those administered empty virus. By analyzing RNA-Seq data and the Targetscan database, we found 9 candidate target genes of miR-874-3p, including ADAM19 (Figure 3A).

In line with the downregulation of miR-874-3p in AC mouse model, ADAM19 was upregulated at the same time points after injury (Figure S6A). Moreover, ADAM19 expression was markedly reduced in AC mice treated with miR-874-3p mimic, compared with mice treated with empty virus (Figure 3B and 3C). Additionally, treatment with miR-874-3p mimic suppressed the expression of ADAM19 in HK2 cells (Figure 3D and S6B). These results could be replicated in the UUO model (Figure S6C through S6E).

We further analyzed 2 predicted miR-874-3p target sites in the human *ADAM19* gene by performing a luciferase reporter assay. MiR-874-3p repressed ADAM19 luciferase expression in the presence of the plasmid containing the site 1 sequence but did not affect luciferase expression in the presence of the plasmid containing the mutated site 1 sequence and site 2 sequence (Figure 3E), suggesting that miR-874-3p directly targets site 1 and represses ADAM19 expression.

Moreover, ADAM19 was increased in PBMCs from AC mice (Figure S6F). Staining of renal section showed during renal fibrosis, ADAM19 was also expressed in renal proximal tubules and injured tubules (Figure S7). Quantification of ADAM19 staining in human renal biopsy samples of IgAN patients showed that ADAM19 was increased in patients with Lee class III and IV compared with the IgAN patients graded as Lee class I and II (Figure 3F).

ADAM19 Induces Macrophage Infiltration to Promote Renal Fibrogenesis

To determine the role of ADAM19 in renal fibrogenesis, we overexpressed ADAM19 in mouse kidneys using adenovirus carrying the GFP-labeled mouse *Adam19* coding sequence (Figure 4A, Figure S8A and S8B). The mRNA expression of several fibrotic genes, including *Acta2*, *Col1a1*, and *Fn1*, was augmented 15 days after administration of the ADAM19 adenovirus (Figure 4B). Immunofluorescent analysis revealed that cells overexpressed ADAM19 (GFP^+) was adjacent to tubular epithelial cells, and was colocalized with fibrocytes (type I collagen$^+$ α-SMA^+) and macrophages ($F4/80^+$; Figure 4C, Figures S8C and S9). In consistent with qPCR results, expression of type I collagen (Collagen I or Col-I), α-SMA was increased by ADAM19 overexpression. The flow cytometry analysis showed increased macrophage infiltration in mice treated with ADAM19 adenovirus (Figure 4D), in line with the effect of decreasing miR-874-3p. Again, these results were consistent with mice overexpressed ADAM19 by adenovirus carrying the human *ADAM19* coding sequence (Figure S10).

To assess the role of macrophages in renal fibrosis, clodronate liposomes were administered to deplete macrophages in mice overexpressing ADAM19 (Figure 4E and S11A). The fibrogenic effects of ADAM19 overexpression were abrogated following macrophage depletion (Figure 4F; Figure S11B and S11C).

MiR-874-3p/ADAM19 Mediates CCL2 Expression Through Notch1 Activation

The RNA-Seq analysis showed that the pathways enriched from miR-874-3p mimic treatment were primarily related to cytokine-cytokine receptor interactions and chemokine signaling pathways in UUO mice (Figure 5A). CCL2 is a key chemotactic protein that recruits circulatory monocytes and tissue macrophages in renal injury and fibrosis.[31,32] By qPCR and Western blot, we found that CCL2 expression in kidney was downregulated in AC mice treated with miR-874-3p mimic (Figure 5B and Figure S12A), and increased in

Figure 4 Continued. labeled renal proximal tubules. KIM-1 (violet, yellow arrows) marked injured tubules. DAPI (blue) is a stain for nucleic acid. Scale bar, 100 and 20 μm. Quantification of immunostaining showed expression of KIM-1, α-SMA, Col-I, and F4/80 increased in mice treated with ADAM19 virus. Sham, n=3; empty virus, n=4; ADAM19, n=4; *P<0.05, **P<0.01, ***P<0.001. **D**, Flow cytometry analysis showed increased renal macrophage infiltration in mice treated with ADAM19 adenovirus. n=3 for empty virus and n=4 for ADAM19. *P<0.05, vs empty virus. **E**, Experimental design of the treatment procedure. Clodronate liposomes were delivered to the mice through ophthalmic vein injection every 4 d, whereas adenoviruses encoding human ADAM19 or empty viruses were delivered to mice through kidney injection. **F**, Masson trichrome staining of renal sections showed less fibrosis in mice overexpressing ADAM19 treated with clodronate liposomes than PBS-liposomes. Scale bar, 100 μm. **P<0.01 vs empty virus. Data were expressed as means±SEM. Student *t* test was for (**D**); One-way ANOVA and Tukey post hoc test were used for (**B**) and (**C**).

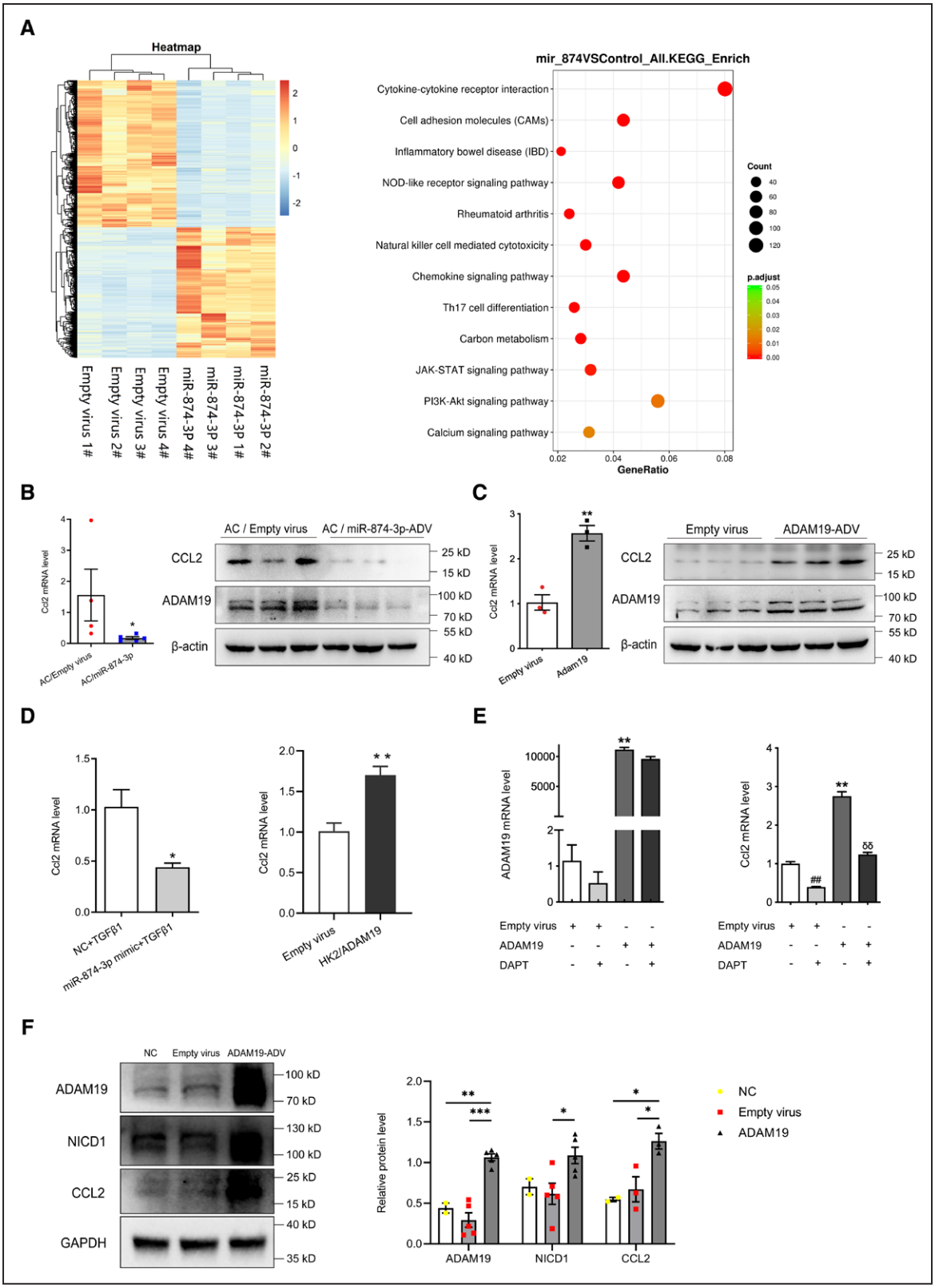

Figure 5. MicroRNA (MiR)-874-3p/ADAM (A Disintegrin and Metalloprotease) 19 mediates CCL2 expression through Notch1 activation.

A, Heatmap of differentially expressed mRNAs in unilateral ureteral obstruction mice treated with miR-874-3p adenovirus or empty virus. KEGG Pathway enrichment analysis and functional analysis showed cytokine-cytokine receptor interaction and chemokine signaling pathways enriched in mice kidneys treated with miR-874-3p adenovirus. **B**, Decreased CCL2 expression in acute-chronic (AC) mice treated with miR-874-3p adenovirus, relative to those treated with empty virus. Empty virus n=4, miR-874-3p, n=5. *P<0.05 vs empty virus. (*Continued*)

mice treated with ADAM19 virus (Figure 5C and Figure S12B). MiR-874-3p mimic also attenuated CCL2 expression induced by treatment with TGF-β1 in HK2 cells in vitro (Figure 5D). In contrast, ADAM19 overexpression increased *CCL2* mRNA expression in HK2 cells (Figure 5D). These observations were confirmed in UUO mice treated with miR-874-3p mimic (Figure S12A and S12B). Collectively, these results indicated that miR-874-3p/ADAM19 regulates CCL2 expression, thereby affecting macrophage infiltration during renal fibrosis.

ADAM proteases are essential for the cleavage and activation of the Notch receptor,[33] and Notch1 has been proved as an upstream regulator of CCL2.[34] We found that Notch1 was upregulated in UUO mice but downregulated in UUO mice treated with miR-874-3p mimic (Figure S12C and S12D). Based on these findings, we speculated that ADAM19 may increase CCL2 expression via the activation of the Notch signaling pathway. To study this, we overexpressed ADAM19 in rat renal tubular cells (NRK-52E) using an adenoviral vector and found that the levels of NICD1 (Notch receptor intracellular domain 1) and CCL2 were increased (Figure 5F). The Notch1 pathway antagonist N-(N-[3,5-difluorophenacetyl]-L-alanyl)-S-phenylglycine t-butyl ester, a γ secretase inhibitor, decreased *Ccl2* mRNA in NRK-52E cells treated with ADAM19 adenovirus (Figure 5E). N-(N-[3,5-difluorophenacetyl]-L-alanyl)-S-phenylglycine t-butyl ester did not affect ADAM19 expression, indicating that ADAM19 is upstream of Notch1 pathway.

Immunofluorescence showed more renal NICD1 staining in renal tubular epithelial cells in mice treated with ADAM19 adenovirus than those with empty virus, accompanied by α-SMA$^+$ cells infiltration in the tubulointerstitial area (Figure 6A and 6B). We further examined the Notch signaling activation in mice treated with ADAM19 adenovirus and found that the mRNA expression of *Notch1*, *Hes1* (hes family bHLH transcription factor 1), and *Dll4* (delta like canonical Notch ligand 4) was enhanced (Figure 6D).

Taken together, miR-874-3p/ADAM19 mediates renal fibrosis after AKI by increasing macrophage infiltration via the Notch1/CCL2 pathway.

DISCUSSION

In current study, we show that miR-874-3p/ADAM19 plays a crucial role in mediating renal fibrosis. Renal fibrosis is associated with downregulation of miR-874-3p in both renal cells and PBMCs. As a critical target of miR-874-3p, ADAM19 expression is augmented after AKI, which enhances CCL2 production via cleavage and activation of Notch1 pathway. To the best of our knowledge, it is the first time to demonstrate that miR-874-3p/ADAM19 mediates the development of renal fibrosis after AKI by regulating macrophage infiltration.

MiR-874-3p was significantly downregulated in renal fibrosis after AKI, soon after the onset of the AC or UUO model. This indicates that miR-874-3p is involved in the early stage of renal fibrosis, probably even in the initial stages of renal injury. Yao et al[35] previously reported that miR-874-3p alleviates renal injury and inflammatory responses in diabetic nephropathy by targeting toll-like receptor-4. Here, we found that miR-874-3p suppresses CCL2 expression and macrophage infiltration and attenuates renal fibrosis by decreasing ADAM19, strongly suggesting a therapeutic potential for miR-874-3p in the treatment of renal fibrosis. Our study also shows that miR-874-3p expression in peripheral blood mononuclear cells of IgAN patients with severe classes was decreased, along with increased expression of ADAM19 in the kidney of the same human cohort. Because miRs are stable and easily detected,[36] miR-874-3p could also serve as a blood marker to detect renal fibrosis.

Our RNA-seq and following study established ADAM19 as a pivotal target of miR-874-3p in the development of renal fibrosis. Our histological results confirmed the renal expression of ADAM19 and were consistent with previous findings from other models. Study by Melenhorst et al[20] showed that kidney expresses a large amount of ADAM19 during embryonic development, and it is mainly located in the glomerular endothelial cells, mesangium, renal tubules, and collecting ducts. After birth, ADAM19 is mainly expressed in vascular endothelial cells. Only a small number of distal tubules have been shown to express ADAM19 but not in proximal tubules. Ramdas et al[37] have shown that ADAM19 is highly expressed in renal tubular epithelial cells after TGF-β treatment in vitro

Figure 5 Continued. **C**, CCL2 expression was increased in the mice treated with ADAM19 adenovirus than those with empty virus. ADAM19 and empty virus, n=3/group. ***P*<0.01 vs empty virus. **D**, Transfection of miR-874-3p mimic into HK2 cells treated with TGF (transforming growth factor)-β1 (10 ng/mL, 24 h) reduced CCL2 mRNA expression. **P*<0.05. CCL2 expression was increased in HK2 cells treated with ADAM19 adenovirus. n=3 for each group, ***P*<0.01 vs empty virus. **E**, The *ADAM19* and *CCL2* mRNA levels in NRK-52E cells treated with ADAM19 adenovirus or empty virus, with/without Notch1 pathway antagonist N-(N-[3,5-difluorophenacetyl]-L-alanyl)-S-phenylglycine t-butyl ester (DAPT). n=3 for each group; ##*P*<0.01, empty virus with DAPT vs empty virus without DAPT; δδ*P*<0.01, ADAM19 adenovirus with DAPT vs ADAM19 adenovirus without DAPT; ***P*<0.01, ADAM19 vs empty virus groups. **F**, Transfection of adenovirus carrying *ADAM19* into NRK-52E cells induced the expression of NICD1 (Notch receptor intracellular domain 1) and CCL2 proteins. The relative protein levels were analyzed by gray levels and normalized to total protein level. Data were pooled from at least two independent experiments. In ADAM19 and NICD1, n=2 for NC, n=5 for empty virus and ADAM19 groups, ***P*<0.01 and ****P*<0.001. In CCL2, n=2 for NC, n=3 for empty virus and ADAM19 groups, **P*<0.05. Data were expressed as means±SEM. Student *t* test was for (**C**), (**D**), and (**E**). Mann-Whitney *U* test was for (**B**). One-way ANOVA and Tukey post hoc test were used for (**F**).

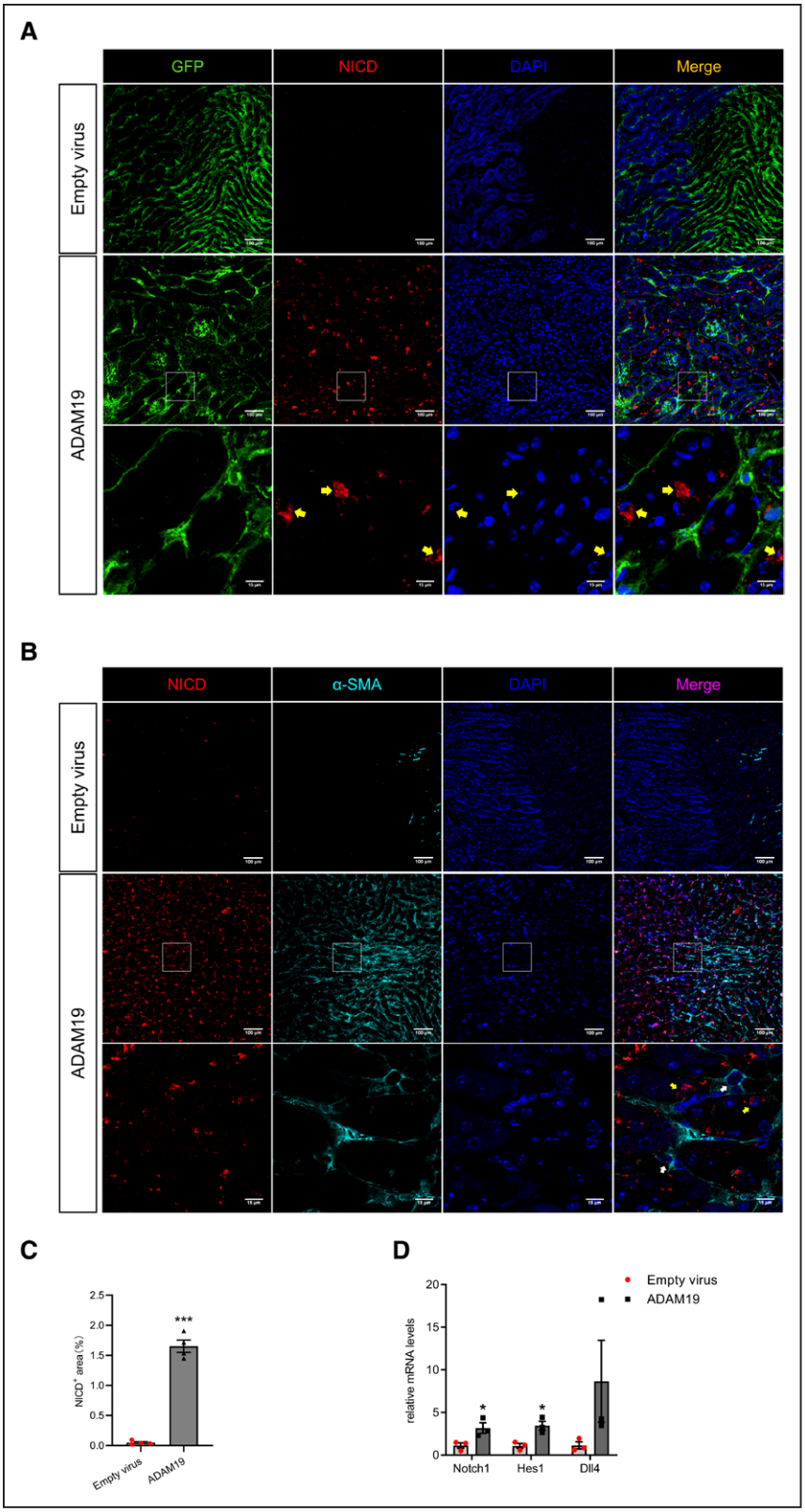

Figure 6. ADAM (A Disintegrin and Metalloprotease) 19 overexpression induces NICD1 (Notch receptor intracellular domain 1) expression in mice.

A and **B**, Representative images of immunofluorescence showed more renal NICD1 staining (red, yellow arrows) in renal tubular epithelial cells in mice treated with ADAM19 adenovirus (GFP [green fluorescent protein], green) than those with empty virus, accompanied with α-SMA$^+$ (α-smooth muscle actin; turquoise, white arrows) cells infiltration in the tubulointerstitial area. DAPI is a stain for nucleic acid. Scale bar, 100 μm and 15 μm. **C**, Quantification of immunostaining showed NICD1 expression increased in mice treated with ADAM19 virus. ADAM19 and empty virus, n=4/group. ***P<0.001. **D**, Notch signaling was activated in mice treated with ADAM19 adenovirus. n=3/group. *P<0.05, vs empty virus. Data were expressed as means±SEM. Student t test was for (**C**) and (**D**).

and specifically expressed in the epithelial cells of the dilated tubules in UUO model. Besides, we also found ADAM19 is expressed in PBMC during renal fibrosis. ADAM19 is a transmembrane protein and has an extracellular metalloproteinase domain that catalytically mediates ectodomain shedding of substrates, including cytokines, growth factors, receptors, and cell adhesion molecules.[20,21] In current study, ADAM19 was transduced and expressed nonspecifically in renal tissue with our adenoviral vector but was primarily detected in interstitial

cells. Overexpression of ADAM19 might change the inflammatory milieu via functioning on extracellular substrates, and promote renal fibrosis.

We further show that ADAM19 promotes renal inflammation and renal fibrosis by cleavage and activation of Notch1. Being known as an upstream regulator of CCL2, Notch1 plays a crucial role in macrophage activation and infiltration, thereby accentuating inflammatory response, leading to chronic inflammation and tissue fibrosis.[34,38] The Notch signaling pathway is also instrumental in cell differentiation and fate determination.[39] In this process, the role of ADAM protease is indispensable. Studies on Drosophila and mammals have found that Notch-mediated signal transduction is caused by the conformational change of Notch heterodimer, and this conformational change can be induced by cleavage of Notch receptors from ADAM10 or ADAM17 on cell membrane.[40–42] Although both ADAM10 and ADAM17 can cleave Notch in in vitro experiments, knockout mouse models have shown that Notch is primarily shedded by ADAM10 in vivo.[21] Our study indicated a novel cleavage mechanism of Notch1 by ADAM19. However, further validation needs to be performed in knockout mouse models.

In conclusion, we show that the miR-874-3p/ADAM19 pathway regulates renal fibrogenesis after AKI. These findings not only provide new insights into the mechanisms underlying renal fibrosis but also offer potential therapeutic targets for treating this disease.

PERSPECTIVES

The progression of kidney damage and hypertension is closely related to renal histological fibrosis in CKD patients. There is a strong association between AKI and the subsequent development of CKD and hypertension. Inflammation and maladaptive repair are of vital importance during the pathogenesis of CKD after AKI; however, the mechanism involved remains unclear. In this study, miR-874-3p was found to be reduced in mouse models of renal fibrosis induced by I/R or obstruction and in human peripheral blood mononuclear cells of IgA nephropathy patients of severe pathological classes. Overexpression of miR-874-3p in vivo alleviated renal fibrosis and reduced macrophage infiltration through decreasing the expression of ADAM19. In addition, overexpression of ADAM19 directly induces renal fibrosis and macrophage infiltration via Notch1/CCL2 pathway. These findings suggest novel insights into the potential therapeutic target and diagnostic biomarker of renal fibrosis.

ARTICLE INFORMATION

Received December 31, 2020; accepted February 11, 2021.

Affiliations

Kidney Disease Center, The First Affiliated Hospital (J.W., W.N., X.X., M.B., Y.M., L.J., L.X., Y.Y., J.C., W.L., F.H.) and Institute of Translational Medicine, Zhejiang University School of Medicine, Hangzhou, China (M.B., P.S., W.L.). Institute of Nephrology, Zhejiang University, Hangzhou, China (J.W., W.N., X.X., M.B., Y.M., L.J., L.X., Y.Y., J.C., W.L., F.H.). Key Laboratory of Kidney Disease Prevention and Control Technology, Zhejiang Province, Hangzhou, China (J.W., W.N., X.X., M.B., Y.M., L.J., L.X., Y.Y., J.C., W.L., F.H.). Department of Medicine, School of Medicine and Health Sciences, The George Washington University, Washington, DC (P.A.J., I.A.).

Acknowledgments

We acknowledge Dr Xiao Shen from Zhejiang University School of Medicine for suggestions in designing the study. F. Han and W. Lin developed the hypothesis and research idea, designed the study, and wrote the article; J. Wang and W. Nie performed the experiments, analyzed the data, and drafted the article; X. Xie did the acute-chronic (AC) mouse model and part of the animal experiments; M. Bai, Y. Ma, L. Jin, and Y. Yang did part of the experiments; L. Xiao, P. Shi, I. Armando, P.A. Jose, and J. Chen helped in the revision of the article.

Sources of Funding

This study was supported by the funds from Primary Research and Development Plan of Zhejiang Province (2020C03034) to F. Han and National Natural Science Foundation of China (81570605, 81770674, 81670651, 81970573) to F. Han and W. Lin.

Disclosures

None.

REFERENCE

1. Ku E, Lee BJ, Wei J, Weir MR. Hypertension in CKD: core curriculum 2019. *Am J Kidney Dis*. 2019;74:120–131. doi: 10.1053/j.ajkd.2018.12.044
2. Wilson S, Mone P, Jankauskas SS, Gambardella J, Santulli G. Chronic kidney disease: definition, updated epidemiology, staging, and mechanisms of increased cardiovascular risk [published online January 17, 2021]. *J Clin Hypertens (Greenwich)*. doi: 10.1111/jch.14186
3. Mattson DL. Immune mechanisms of salt-sensitive hypertension and renal end-organ damage. *Nat Rev Nephrol*. 2019;15:290–300.
4. Hoste EAJ, Kellum JA, Selby NM, Zarbock A, Palevsky PM, Bagshaw SM, Goldstein SL, Cerdá J, Chawla LS. Global epidemiology and outcomes of acute kidney injury. *Nat Rev Nephrol*. 2018;14:607–625. doi: 10.1038/s41581-018-0052-0
5. Chawla LS, Eggers PW, Star RA, Kimmel PL. Acute kidney injury and chronic kidney disease as interconnected syndromes. *N Engl J Med*. 2014;371:58–66. doi: 10.1056/NEJMra1214243
6. Coca SG, Yusuf B, Shlipak MG, Garg AX, Parikh CR. Long-term risk of mortality and other adverse outcomes after acute kidney injury: a systematic review and meta-analysis. *Am J Kidney Dis*. 2009;53:961–973. doi: 10.1053/j.ajkd.2008.11.034
7. Chawla LS, Kimmel PL. Acute kidney injury and chronic kidney disease: an integrated clinical syndrome. *Kidney Int*. 2012;82:516–524. doi: 10.1038/ki.2012.208
8. Zwiers AJM, IJsselstijn H, van Rosmalen J, Gischler SJ, de Wildt SN, Tibboel D, Cransberg K. CKD and hypertension during long-term follow-up in children and adolescents previously treated with extracorporeal membrane oxygenation. *Clin J Am Soc Nephrol*. 2014;9:2070–2078.
9. Kumar S. Cellular and molecular pathways of renal repair after acute kidney injury. *Kidney Int*. 2018;93:27–40. doi: 10.1016/j.kint.2017.07.030
10. Lagos-Quintana M, Rauhut R, Lendeckel W, Tuschl T. Identification of novel genes coding for small expressed RNAs. *Science*. 2001;294:853–858. doi: 10.1126/science.1064921
11. Trionfini P, Benigni A, Remuzzi G. MicroRNAs in kidney physiology and disease. *Nat Rev Nephrol*. 2015;11:23–33. doi: 10.1038/nrneph.2014.202
12. Brandenburger T, Salgado Somoza A, Devaux Y, Lorenzen JM. Noncoding RNAs in acute kidney injury. *Kidney Int*. 2018;94:870–881. doi: 10.1016/j.kint.2018.06.033
13. Guo C, Dong G, Liang X, Dong Z. Epigenetic regulation in AKI and kidney repair: mechanisms and therapeutic implications. *Nat Rev Nephrol*. 2019;15:220–239. doi: 10.1038/s41581-018-0103-6
14. Trionfini P, Benigni A. MicroRNAs as master regulators of glomerular function in health and disease. *J Am Soc Nephrol*. 2017;28:1686–1696. doi: 10.1681/ASN.2016101117
15. Baker MA, Davis SJ, Liu P, Pan X, Williams AM, Iczkowski KA, Gallagher ST, Bishop K, Regner KR, Liu Y, et al. Tissue-specific MicroRNA expression

patterns in four types of kidney disease. *J Am Soc Nephrol*. 2017;28:2985–2992. doi: 10.1681/ASN.2016121280
16. Nieto MA, Huang RY, Jackson RA, Thiery JP. EMT: 2016. *Cell*. 2016;166:21–45. doi: 10.1016/j.cell.2016.06.028
17. Li X, Pan X, Fu X, Yang Y, Chen J, Lin W. MicroRNA-26a: an emerging regulator of renal biology and disease. *Kidney Blood Press Res*. 2019;44:287–297. doi: 10.1159/000499646
18. Han F, Konkalmatt P, Chen J, Gildea J, Felder RA, Jose PA, Armando I. MiR-217 mediates the protective effects of the dopamine D2 receptor on fibrosis in human renal proximal tubule cells. *Hypertension*. 2015;65:1118–1125. doi: 10.1161/HYPERTENSIONAHA.114.05096
19. Gerlach CV, Vaidya VS. MicroRNAs in injury and repair. *Arch Toxicol*. 2017;91:2781–2797. doi: 10.1007/s00204-017-1974-1
20. Melenhorst WB, van den Heuvel MC, Timmer A, Huitema S, Bulthuis M, Timens W, van Goor H. ADAM19 expression in human nephrogenesis and renal disease: associations with clinical and structural deterioration. *Kidney Int*. 2006;70:1269–1278. doi: 10.1038/sj.ki.5001753
21. Lambrecht BN, Vanderkerken M, Hammad H. The emerging role of ADAM metalloproteinases in immunity. *Nat Rev Immunol*. 2018;18:745–758. doi: 10.1038/s41577-018-0068-5
22. Melenhorst WB, van den Heuvel MC, Stegeman CA, van der Leij J, Huitema S, van den Berg A, van Goor H. Upregulation of ADAM19 in chronic allograft nephropathy. *Am J Transplant*. 2006;6:1673–1681. doi: 10.1111/j.1600-6143.2006.01384.x
23. Arai HN, Sato F, Yamamoto T, Woltjen K, Kiyonari H, Yoshimoto Y, Shukunami C, Akiyama H, Kist R, Sehara-Fujisawa A. Metalloprotease-dependent attenuation of BMP signaling restricts cardiac neural crest cell fate. *Cell Rep*. 2019;29:603–616.e5.
24. Lee SM, Rao VM, Franklin WA, Schiffer MS, Aronson AJ, Spargo BH, Katz AI. IgA nephropathy: morphologic predictors of progressive renal disease. *Hum Pathol*. 1982;13:314–322. doi: 10.1016/s0046-8177(82)80221-9
25. Xiao L, Zhou D, Tan RJ, Fu H, Zhou L, Hou FF, Liu Y. Sustained activation of Wnt/β-catenin signaling drives AKI to CKD progression. *J Am Soc Nephrol*. 2016;27:1727–1740.
26. Bao YW, Yuan Y, Chen JH, Lin WQ. Kidney disease models: tools to identify mechanisms and potential therapeutic targets. *Zool Res*. 2018;39:72–86. doi: 10.24272/j.issn.2095-8137.2017.055
27. Wang P, Luo M-L, Song E, Zhou Z, Ma T, Wang J, Jia N, Wang G, Nie S, Liu Y, Hou FF. Long noncoding RNA lnc-TSI inhibits renal fibrogenesis by negatively regulating the TGF-β/Smad3 pathway. *Sci Transl Med*. 2018;10:eaat2039. doi: 10.1126/scitranslmed.aat2039.
28. Ke QF, Wang LX. Neuroanatomical evidence of the melanocortin-4 receptor expression in the mesencephalic periaqueductal gray innervating renal tissues. *Int J Clin Exp Med*. 2015;8:6119–6123.
29. Fu X, Jin L, Wang X, Luo A, Hu J, Zheng X, Tsark WM, Riggs AD, Ku HT, Huang W. MicroRNA-26a targets ten eleven translocation enzymes and is regulated during pancreatic cell differentiation. *Proc Natl Acad Sci USA*. 2013;110:17892–17897. doi: 10.1073/pnas.1317397110
30. McAdoo SP, Bhangal G, Page T, Cook HT, Pusey CD, Tam FW. Correlation of disease activity in proliferative glomerulonephritis with glomerular spleen tyrosine kinase expression. *Kidney Int*. 2015;88:52–60. doi: 10.1038/ki.2015.29
31. Tang PM, Nikolic-Paterson DJ, Lan HY. Macrophages: versatile players in renal inflammation and fibrosis. *Nat Rev Nephrol*. 2019;15:144–158. doi: 10.1038/s41581-019-0110-2
32. Xu L, Sharkey D, Cantley LG. Tubular GM-CSF promotes late MCP-1/CCR2-mediated fibrosis and inflammation after ischemia/reperfusion injury. *J Am Soc Nephrol*. 2019;30:1825–1840. doi: 10.1681/ASN.2019010068
33. Kopan R, Ilagan MX. The canonical Notch signaling pathway: unfolding the activation mechanism. *Cell*. 2009;137:216–233. doi: 10.1016/j.cell.2009.03.045
34. Yumimoto K, Akiyoshi S, Ueo H, Sagara Y, Onoyama I, Ueo H, Ohno S, Mori M, Mimori K, Nakayama KI. F-box protein FBXW7 inhibits cancer metastasis in a non-cell-autonomous manner. *J Clin Invest*. 2015;125:621–635. doi: 10.1172/JCI78782
35. Yao T, Zha D, Gao P, Shui H, Wu X. MiR-874 alleviates renal injury and inflammatory response in diabetic nephropathy through targeting toll-like receptor-4. *J Cell Physiol*. 2018;234:871–879. doi: 10.1002/jcp.26908
36. Pottier N, Cauffiez C, Perrais M, Barbry P, Mari B. FibromiRs: translating molecular discoveries into new anti-fibrotic drugs. *Trends Pharmacol Sci*. 2014;35:119–126. doi: 10.1016/j.tips.2014.01.003
37. Ramdas V, McBride M, Denby L, Baker AH. Canonical transforming growth factor-β signaling regulates disintegrin metalloprotease expression in experimental renal fibrosis via miR-29. *Am J Pathol*. 2013;183:1885–1896. doi: 10.1016/j.ajpath.2013.08.027
38. Shen Q, Cohen B, Zheng W, Rahbar R, Martin B, Murakami K, Lamorte S, Thompson P, Berman H, Zúñiga-Pflücker JC, et al. Notch shapes the innate immunophenotype in breast cancer. *Cancer Discov*. 2017;7:1320–1335. doi: 10.1158/2159-8290.CD-17-0037
39. Lai EC. Notch signaling: control of cell communication and cell fate. *Development*. 2004;131:965–973. doi: 10.1242/dev.01074
40. Hartmann D, de Strooper B, Serneels L, Craessaerts K, Herreman A, Annaert W, Umans L, Lübke T, Illert AL, et al. The disintegrin/metalloprotease ADAM 10 is essential for Notch signalling but not for alpha- secretase activity in fibroblasts. *Hum Mol Genet*. 2002;11:2615–2624.
41. Brou C, Logeat F, Gupta N, Bessia C, LeBail O, Doedens JR, Cumano A, Roux P, Black RA, Israël A. A novel proteolytic cleavage involved in Notch signaling: the role of the disintegrin-metalloprotease TACE. *Mol Cell*. 2000;5:207–216. doi: 10.1016/s1097-2765(00)80417-7
42. Mumm JS, Schroeter EH, Saxena MT, Griesemer A, Tian X, Pan DJ, Ray WJ, Kopan R. A ligand-induced extracellular cleavage regulates gamma-secretase-like proteolytic activation of Notch1. *Mol Cell*. 2000;5:197–206. doi: 10.1016/s1097-2765(00)80416-5